

NASA Technical Memorandum 104353
AIAA-91-1566

1N-02
11707
p19

Numerical Flux Formulas for the Euler and Navier-Stokes Equations

II. Progress in Flux-Vector Splitting

William J. Coirier
*Lewis Research Center
Cleveland, Ohio*

and

Bram van Leer
*University of Michigan
Ann Arbor, Michigan*

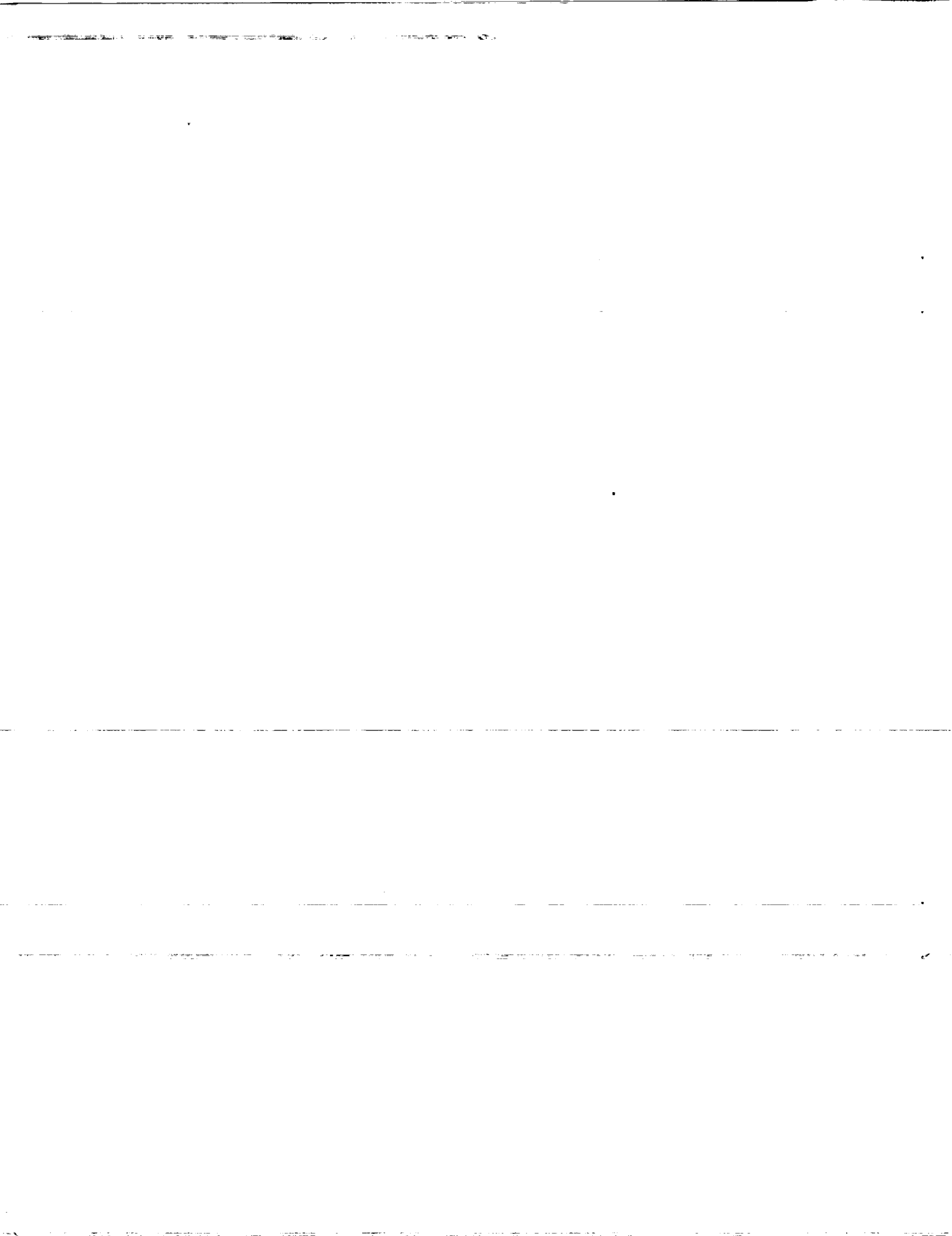
Prepared for the
10th Computational Fluid Dynamics Conference
sponsored by the American Institute of Aerodynamics and Astronautics
Honolulu, Hawaii, June 24-27, 1991

(NASA-TM-104353) NUMERICAL FLUX FORMULAS
FOR THE EULER AND NAVIER-STOKES EQUATIONS.
2: PROGRESS IN FLUX-VECTOR SPLITTING (NASA)
19 p CSCL 01A

N91-22084

Unclas
G3/02 0011707





Numerical Flux Formulas for the Euler and Navier–Stokes Equations

II. Progress in Flux–Vector Splitting

William J. Coirier*

National Aeronautics and Space Administration
Lewis Research Center
Cleveland, Ohio 44135

and

Bram van Leer†

University of Michigan
Department of Aerospace Engineering
Ann Arbor, Michigan 48109-2140

1 Abstract

The accuracy is studied of various numerical flux functions for the inviscid fluxes when used for Navier-Stokes computations. The flux functions are benchmarked for solutions of the viscous, hypersonic flow past a 10° cone at zero angle of attack using first-order, upwind spatial differencing. The Harten-Lax/Roe flux is found to give a good boundary layer representation, although its robustness is an issue. Some hybrid flux formulas, where the concepts of flux-vector and flux-difference splitting are combined, are shown to give unsatisfactory pressure distributions; there is still room for improvement. Investi-

gations of low diffusion, pure flux-vector splittings indicate that a pure flux-vector splitting can be developed that eliminates spurious diffusion across the boundary layer. The resulting first-order scheme is marginally stable and not monotone.

2 Introduction

This paper addresses the problem of designing accurate numerical flux functions approximating the inviscid fluxes in the Euler and Navier-Stokes equations, and may be regarded as a sequel to [1]. In the latter paper it was demonstrated, among other things, that numerical flux functions that do not recognize contact and shear discontinuities grossly exaggerate the diffusion of entropy and shear

*Graduate Student, Aerospace Engineer, Member AIAA

†Professor, Member AIAA

across the boundary layer in a Navier-Stokes calculation. Specifically, flux formulas of the flux-vector splitting (FVS) type, such as Van Leer's [2], and those based on a tuned scalar viscosity coefficient, such as Jameson's [3], were found to be inferior to those based on flux-difference splitting (FDS), such as Roe's [4].

Since the appearance of [1], a clear shift in the use of the various flux formulas has been observed. FVS is gradually being phased out as a component of Navier-Stokes codes in favor of FDS, while the scalar viscosity coefficient in central-difference schemes on occasion, [5], has been replaced by a viscosity *matrix*, yielding the same low diffusion as FDS.

Another trend, inspired by developments in hypersonic flight, has been the extension of known flux formulas for ideal gases to real and reacting gases. Examples can be found in [6, 7, 8].

At the same time, a growing effort is being spent on the development of genuinely multi-dimensional schemes, in which the influence of the grid coordinate directions is reduced as much as possible. This brings along the formulation of multi-dimensional flux functions, such as the one due to Rumsey et al. [9, 10], which is based on an approximate Riemann solver including waves traveling in two orthogonal directions of physical importance. Another example is the one by Goorjian and Obayashi [11], based on waves traveling in and normal to the flow direction.

Independent of the above developments, several attempts have still been made to salvage the concept of FVS, mainly because of three reasons:

1. the formulas are relatively simple;
2. the split fluxes are easy to linearize, for the benefit of implicit marching schemes.
3. the extension to real gases is relatively straightforward

Worth mentioning in this field is the work of Hänel [12, 13], who has suggested a number of modifications to Van Leer's [2] FVS, including a mix with FDS formulas. This hybrid approach was carried further by Van Leer [14] and appears to be completed by Liou and Steffen [15], whose AUSM (Advective Upwind Splitting Method) flux appears to rival the accuracy and robustness of Roe's at significantly reduced computational complexity.

In the present paper we review some of these new developments in FVS, and subsequently pose the following question:

- *Is it possible at all to construct a pure FVS that does not diffuse a grid-aligned boundary layer, and makes a stable combination with some form of time-marching?*

The answer turns out to be "yes," but loss of monotonicity of the numerical solution is unavoidable.

Thus, improvements to date of the original Van Leer FVS can be grouped into two categories:

- "Hybrid", or mixed FVS/FDS modifications
- "Pure" FVS modifications

To compare the accuracy of the various flux functions when used for a viscous computation, the viscous, hypersonic flow over a cone at zero angle of attack is used to benchmark the flux formulas. In keeping with the style of the earlier paper, [1], we present solutions for the Mach 7.95 viscous flow over a 10° cone at a Reynolds number of $Re_L = 0.42 \times 10^6$ and freestream total temperature of $T_{0,\infty} = 775.56K$. Adiabatic wall boundary conditions are applied at the cone surface, resulting in a wall temperature of $T_w = 11.73T_\infty$ and a boundary layer thickness of approximately 0.5° . In contrast to the

approach in [1], which used a two-dimensional code for the flux comparisons, we solve the one-dimensional conical Navier-Stokes equations. In all of the following computations, the residual is formed using first-order upwind differencing with the various flux functions. Unless otherwise noted, Yoon’s [16] LU-SGS scheme for approximate Newton iteration is used to obtain the solutions. All of the computations reported here were made on a uniform mesh composed of 50 cells spanning 5° from the cone surface. For the benchmark cases, this results in approximately 8 points in the boundary layer. The Harten-Lax/Roe flux that was presented, but not tested, in [1] is compared to Roe’s FDS scheme for the conical flow in Section 3. Section 4 outlines recent hybrid modifications to the original FVS scheme and compares these to the original FVS and Roe’s FDS scheme for the conical flowfield. Section 5 addresses the prospect of pure FVS splitting and shows that, although the adverse dissipative properties of the original scheme can be negated, the resulting flux formulas are non-monotone. This non-monotonicity is shown to be unavoidable, and is evident from an examination of the eigenvalues of the split flux Jacobians as well as the eigenvalues of a linearized representation of the residual.

3 Harten-Lax/Roe Flux

The Harten-Lax/Roe flux ([17] and [18]) is an FDS formula, incorporating a “smart” scalar dissipation coefficient: the scalar is a square-amplitude weighted average of the characteristic speeds. This formula was discussed in [1], but not tested. The Harten-Lax/Roe flux does not yield linear stability, as the scalar dissipation coefficient may be too small for stabilizing the weaker waves with the larger characteristic speeds. The instability will show up first in these waves, increasing their

amplitude, which then feeds back into the dissipation coefficient, increasing its value; thus, stability is restored.

Numerical solutions for the temperature and the pressure are shown in Figures 1 and 2; for comparison the results of our benchmark flux, i.e. Roe’s [4], are also given. As can be seen from the figures, agreement with the benchmark results is excellent, although very minor pressure oscillations are observed in the boundary layer. The presence of these oscillations might indicate a tendency towards a non-linear instability that could show up in a more demanding calculation. Convergence was readily achieved with the LU-SGS scheme using an infinite Courant number. Convergence was also achieved using a single stage explicit (forward Euler) scheme, but a very small Courant number was needed. This convergence behavior was found on a range of 32-bit machines, while on two 64-bit machines (CRAY Y-MP and X-MP), this flux combined with either the LU-SGS or forward Euler scheme yielded only a three order of magnitude drop in the L_2 norm of the residual. The Harten-Lax/Roe flux nominally uses all of the wave strengths and speeds evaluated at Roe’s averaged state, but blends these into a single, weighted wave speed for the construction of the numerical flux. It is only a small step computing Roe’s flux once the wave strengths and speeds are found, and one might as well go all the way, and compute the flux using Roe’s formula. As pointed out in the previous paper [1], though, the weighted speed can be obtained more simply as a ratio of scalar products:

$$V = \frac{\Delta \mathbf{W} \circ \Delta \mathbf{F}}{\Delta \mathbf{W} \circ \Delta \mathbf{U}} \quad (1)$$

where \mathbf{U} is the vector of conserved state quantities, \mathbf{F} is the flux vector, and \mathbf{W} is an alternative state vector, *viz.* the gradient of an entropy function associated with the Euler equations; for instance $\mathbf{W} = \frac{\partial(-\rho S)}{\partial \mathbf{U}}$. In spite

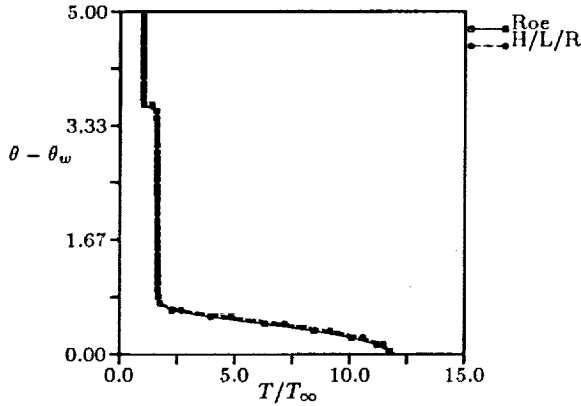


Figure 1: Conical Navier-Stokes solution using Harten/Lax/Roe's scheme; temperature distributions.

of this simplification, this ingenious scheme might not obtain the notoriety that Roe's scheme has obtained because of the stability hazard.

4 Hybrid Modifications of Van Leer's FVS

We recall the definition of FVS:

$$\mathbf{F}(\mathbf{U}) = \mathbf{F}^+(\mathbf{U}) + \mathbf{F}^-(\mathbf{U}); \quad (2)$$

here \mathbf{U} is the vector of conserved state quantities, $\mathbf{F}(\mathbf{U})$ is the vector of inviscid fluxes in one coordinate direction, and $\mathbf{F}^+(\mathbf{U})$ and $\mathbf{F}^-(\mathbf{U})$ are called the forward and backward fluxes, respectively.

The FVS used most frequently in practice is Van Leer's [2], owing to the following design features:

1. The split fluxes are continuously differentiable, which preserves the numerical accuracy near sonic points, and allows smooth linearization;

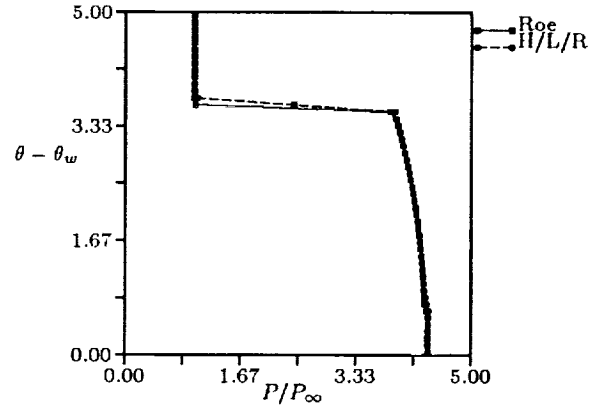


Figure 2: Same solution as in Figure 1; pressure distributions.

2. For subsonic flow, the Jacobians $d\mathbf{F}^+/d\mathbf{U}$ and $d\mathbf{F}^-/d\mathbf{U}$ have a zero eigenvalue, which accounts for crisp numerical profiles of steady shocks.

If the second constraint is relaxed, a one-parameter family of continuously differentiable split fluxes can be generated [6]; these are the simplest possible in the sense that they are at most quartic in the Mach number, just as the Van Leer fluxes. The differences among members of this family arise only in the energy-flux splitting.

Included in this family is the energy-flux splitting originally proposed by Hänel [12]:

$$F_{\text{energy}}^{\pm} = F_{\text{in}}^{\pm} H, \quad (3)$$

where H is the specific total enthalpy. Advantages of this formula are:

1. it is as simple as can be;
2. it admits steady Euler solutions with constant total enthalpy throughout the flow.

Hänel claims that this flux splitting, when used in Navier-Stokes calculations, gives more accurate total-enthalpy values in the

boundary layer. This may have been observed for the lower flow speeds; in the hypersonic flow regime the improvement is insignificant.

The problem of numerical diffusion across a boundary layer, even when it is aligned with the grid, can easily be understood by rewriting the formulas for the flux of a general scalar function, ϕ . For the inviscid fluxes, ϕ would be replaced by u and H for the convective transverse momentum and energy fluxes, respectively. Letting B denote the bottom, and T denote the top cell:

$$\begin{aligned} (\rho v)\phi &= F_{m,B}^+ \phi_B + F_{m,T}^- \phi_T \\ &= (F_{m,B}^+ + F_{m,T}^-) \frac{\phi_B + \phi_T}{2} \\ &\quad - (F_{m,B}^+ - F_{m,T}^-) \frac{\phi_T - \phi_B}{2} \end{aligned} \quad (4)$$

The first term in these expressions represents a central-differencing flux; numerical diffusion is introduced by the second term. When the net mass flux

$$F_m^{\text{net}} = F_{m,B}^+ + F_{m,T}^- \quad (5)$$

vanishes, this is because of a *cancellation*, not because $F_{m,B}^+$ and $F_{m,T}^-$ vanish individually. As a consequence, the diffusive terms do not vanish with the mass flux.

Hänel [13] has suggested to replace the formula for the transverse-momentum flux by one borrowed from *flux-difference* splitting:

$$(\rho v)u = F_m^{\text{net}} u_{\text{upwind}}, \quad (6)$$

with

$$u_{\text{upwind}} = u_B \quad \text{if } F_m^{\text{net}} \geq 0, \quad (7)$$

$$u_{\text{upwind}} = u_T \quad \text{if } F_m^{\text{net}} < 0. \quad (8)$$

This mixture of flux-vector splitting and flux-difference splitting prevents the numerical broadening of the boundary layer, but can

not improve the accuracy of the wall temperature. It further introduces pressure irregularities across the boundary layer.

The similarity of the transverse momentum and energy fluxes, though, suggests that a further improvement can be obtained by introducing a similar formula for the energy flux, i.e.:

$$(\rho v)H = F_m^{\text{net}} H_{\text{upwind}}, \quad (9)$$

with

$$H_{\text{upwind}} = H_B \quad \text{if } F_m^{\text{net}} \geq 0, \quad (10)$$

$$H_{\text{upwind}} = H_T \quad \text{if } F_m^{\text{net}} < 0. \quad (11)$$

As reported in [14], this removes the error in the wall temperature; unfortunately, the pressure irregularity remains.

The next pair of figures shows the temperature and pressure distributions obtained with the three variations of Van Leer's FVS represented by Equations (3), (6) and (9); for comparison, results for the original Van Leer FVS and for Roe's FDS are included. Use of the first modification of the energy flux, Hänel's energy flux, (equation (3), "Hanel 87" in the Figure), hardly causes any change with respect to using the Van Leer flux; the second modification, Hänel's FDS-like transverse-momentum flux, (equation (6), "Hanel 89" in the Figure), does achieve the proper shrinking of the boundary layer, which also corrects the pressure profile (except for a fluctuation near the wall), but the wall temperature is still wrong. The third modification, Van Leer and Hänel's FDS treatment of both the transverse momentum and energy fluxes, (equations (6) and (9), "VL/H 90" in the Figure), finally corrects the wall temperature, but the pressure fluctuation remains.

The final stage in this sequence of hybrid flux formulas is the technique named AUSM, developed by Liou and Steffen [15], where *all* advective terms in the fluxes are treated using the advective Mach number splitting from the

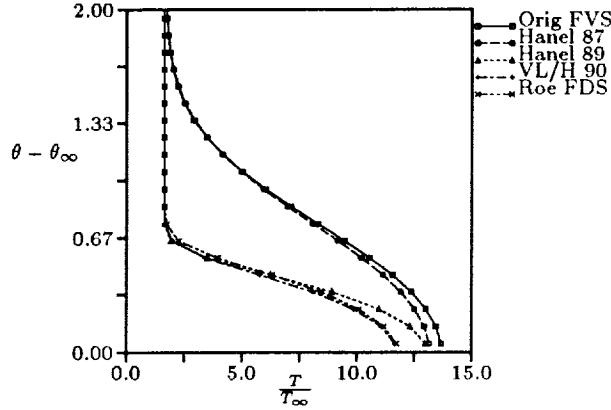


Figure 3: Conical Navier-Stokes solutions using hybrid modifications to the original Van Leer FVS; temperature distributions.

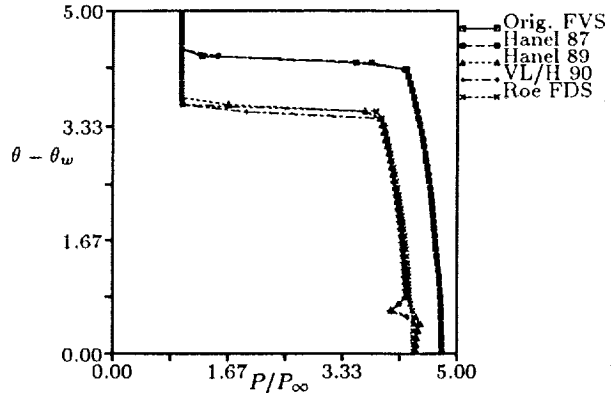


Figure 4: Same solutions as in Figure 3; pressure distributions.

original Van Leer mass splitting. The remaining pressure term is split as usual. Preliminary numerical testing on the cone-flow problem indicates that the results are comparable to those of Roe's flux; in particular, they show a smooth pressure distribution. Some other results are included in the forum-paper by Liou and Steffen [19], included in the present conference proceedings. Since this scheme was not available in the literature at the time that this paper was written, it will not be included in the comparisons made here.

5 Pure FVS Modifications

Unaffected by the development of hybrid FVS/FDS formulas, an intriguing question still remains:

- *Is it possible at all to construct a pure FVS that does not diffuse a grid-aligned boundary layer and makes a stable combination with some form of time-marching?*

This question can be rephrased as:

- *Is it possible to split the Euler fluxes such that both F_m^+ and F_m^- vanish with the flow speed, while numerical stability is maintained?*

If indeed this were possible, the form of the flux splitting for small v would follow immediately from symmetry considerations:

$$F_m^\pm = \frac{1}{2}\rho v + O(v^2), \quad (12)$$

$$F_{\text{mom}\parallel}^\pm = \frac{1}{2}p \pm s\rho av + O(v^2), \quad (13)$$

$$F_{\text{mom}\perp}^\pm = \frac{1}{2}\rho uv + O(v^2), \quad (14)$$

$$F_{\text{energy}}^\pm = \frac{1}{2}\rho H v + O(v^2), \quad (15)$$

where a is the sound speed and s is a free parameter representing the derivative of the split pressures for $v = 0$. Most noticeable is that for $v = 0$ this splitting leads to central differencing, which will be unstable if forward time-differencing is used. If s also vanishes, central differencing will spread to a small neighborhood of $v = 0$. Positive values of s would seem to introduce some dissipation, since this will make the split pressures upwind-biased; this turns out to be not necessarily true. The fluxes (12-15), valid for $v \approx 0$, must smoothly join the branches for larger values of $|v|$; for the latter we may use the standard Van Leer fluxes.

Below we shall study a four-parameter family of splittings of the one-dimensional Euler fluxes, hereafter referred to as Low Diffusion FVS (LDFVS), defined by the formulas, valid for $|M| \leq 1$

$$F_m^\pm = \pm \rho a \left\{ \frac{1}{4}(M \pm 1)^2 - \frac{\mu}{4}(M^2 - 1)^P \right\} \quad (16)$$

$$F_{\text{mom}}^\pm = F_m^\pm v + p^\pm, \quad (17)$$

$$p^\pm = \frac{\rho a^2}{\gamma} \left\{ \frac{1}{4}(M \pm 1)^2 (2 \mp M) \mp \frac{\nu}{4} M (M^2 - 1)^P \right\}, \quad (18)$$

$$F_{\text{energy}}^\pm = F_m^\pm H \mp \omega \rho a^3 M^2 (M^2 - 1)^2 \quad (19)$$

The three chief parameters are μ , ν and ω . If $\mu = \nu = \omega = 0$, the formulas return the standard Van Leer fluxes, with Hänel's energy flux, regardless of the value of P . The higher the value of the exponent P , the narrower the interval around $M = 0$ where the fluxes deviate significantly from the Van Leer-Hänel fluxes. For conciseness, we will only show results for $P = 2$ since the results for higher P are similar in nature. Note that the momentum-splitting is conceived as a split-

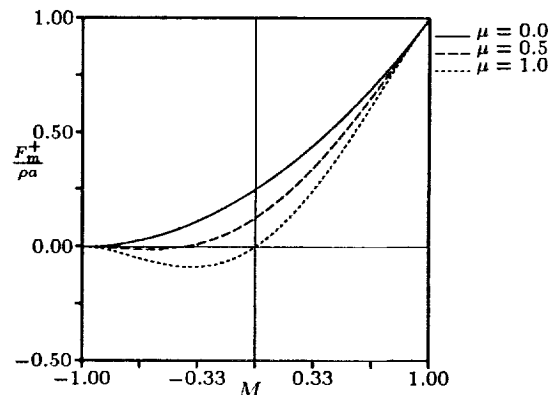


Figure 5: Normalized forward mass flux, $F_m^+ / (\rho a)$, for three values of μ , with $P = 2$.

ting of the convective flux, plus a pressure splitting. The extra terms in the energy splitting are considered less important than those in the mass and momentum fluxes, since the splitting should also be valid for isothermal flow ($\gamma = 1$); in this case the energy equation would drop out completely. Similarly, inclusion of a transverse-momentum flux is not a top priority, since the splittings should be stable in the first place for a one-dimensional flow.

Figures 5, 6 and 7 show the mass, pressure and energy splittings of this family. In Figure 5, three values of the mass splitting parameter, μ , are shown for the forward flux, where $\mu = 0$ results in the original Van Leer splitting and $\mu = 1$ causes the split mass flux to be identically zero at zero Mach number. Note that for the larger values of μ the split flux becomes negative for a range of negative Mach numbers, which is somewhat odd for a "forward" flux, and could be destabilizing.

Figure 6 shows the split pressure from the forward momentum flux. For $\nu = \frac{3}{4}$ the slope of p^+ vanishes at $M = 0$, corresponding to $s = 0$ in Equations (12-15); as mentioned above this leads to central pressure-differencing in the neighborhood of $M = 0$.

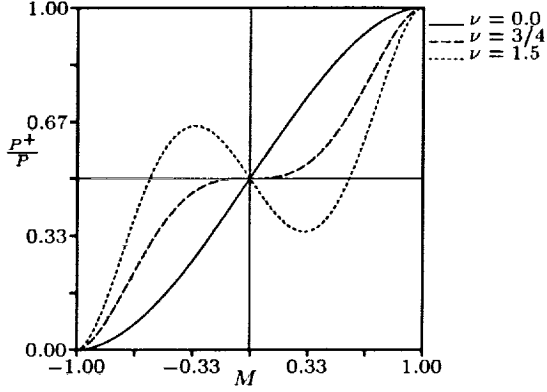


Figure 6: Normalized “forward” pressure, p^+/p , for three values of μ , with $P = 2$.

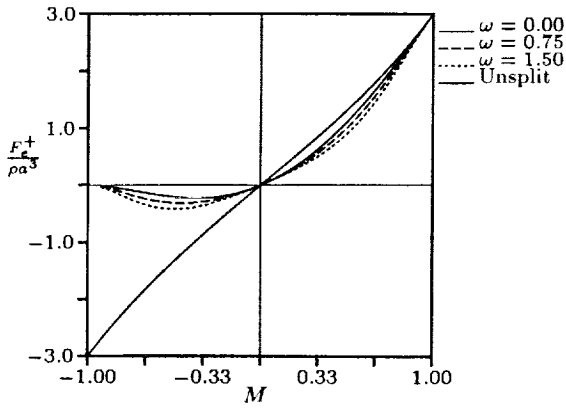


Figure 7: Normalized forward energy flux, $F_{energy}^+ / (\rho a^3)$, for three values of ω .

This value unexpectedly performed well regarding stability. For $\nu > \frac{3}{4}$ the split pressures lose monotonicity, which has little physical appeal; that this is an improper choice is also borne by a stability analysis.

Figure 7 shows the resulting energy splittings for the case of vanishing split mass fluxes at $M = 0$ (i.e. $\mu = 1$), for selected values of the energy-splitting parameter, ω .

Liou and Steffen in [20] have independently derived a pure FVS formula along the same lines as presented above. Their flux has been coined HOPE (for High-Order Polynomial Expansion) and includes splittings that are similar to those presented here. The mass, pressure and energy splittings of the HOPE family are

$$F_m^\pm = \pm \frac{\rho a}{4} \left\{ (M \pm 1)^2 + m_1 (M^2 - 1)^2 \right\} \quad (20)$$

$$F_{mom}^\pm = F_m^\pm v + p^\pm, \quad (21)$$

$$p^\pm = \frac{\rho a^2}{\gamma} \left\{ \frac{1}{4} (M \pm 1)^2 (2 \mp M) \pm m_1 \frac{3}{4} M (M^2 - 1)^2 \right\}, \quad (22)$$

$$F_{energy}^\pm = F_{mass}^\pm H \quad (23)$$

where

$$m_1(M) = (M^2 - 1) / (M^2 + 1)^S \quad (24)$$

A comparison with Eqs. (16-19) shows that the HOPE splitting is very similar to the LD-FVS splitting with $\mu = 1$, $\nu = \frac{3}{4}$ and $\omega = 0$. The function $m_1(M)$ is a blending function that ensures that the split mass flux is zero at $M = 0$ and that the split fluxes smoothly join the unsplit fluxes near $|M| = 1$. As suggested in [20] the parameter S in (24) is taken to be $S = 4$. In [20], various pressure splittings were tested, where the one shown here was found to be the most robust.

Figures 8 and 9 compare mass and pressure splittings of the HOPE and LDFVS families. The effect of the blending function

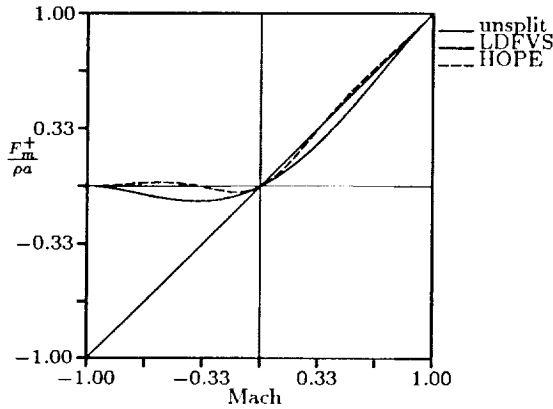


Figure 8: Normalized forward mass flux for the HOPE and LDFVS ($\mu = 1$) splittings.

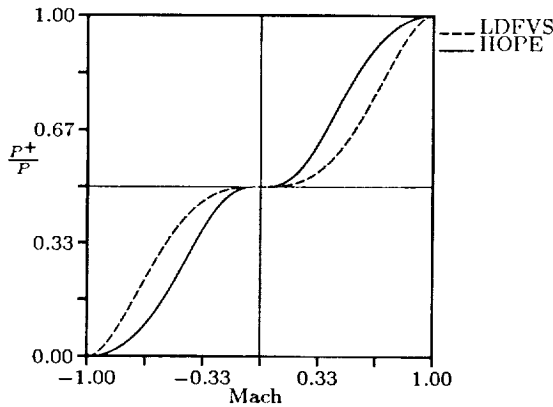


Figure 9: Normalized "forward" pressure flux for the HOPE and LDFVS ($\nu = \frac{3}{4}$) splittings.

in HIOPE is apparent in the Figures. The pressure splittings are much the same, with the HIOPE curve showing a narrower plateau around $M = 0$ and closer agreement with the Van Leer curve near $|M| = 1$. The HIOPE forward mass flux follows the unsplit flux closely for $M > 0$ and oscillates about $F_m^+ = 0$ for $M < 0$, while the LDFVS scheme is overall more smooth. Both pressure and mass splittings of the LDFVS family can be brought close to those of the HIOPE family ($S = 4$) by using a higher exponent P , *viz.* $P = 6$. As will be shown in a following section, the smoothness (or lack of smoothness) of the split fluxes has a direct influence upon the smoothness of the split-flux eigenvalues.

The similarity of the above flux splittings yields comparable stability bounds and, as will be shown in the next section, both fluxes can lead to non-monotone solutions, even with first-order upwind differencing. This non-monotonicity is not readily apparent from the conical flow results shown below, owing in part to the geometric and viscous source terms appearing in the equations, but it appears to be unavoidable in multi-dimensional calculations. Regardless of this unsettling finding, the conical-flow results show that the excess diffusion is eliminated with these flux splittings.

Results obtained with first-order upwind differencing incorporating the LDFVS fluxes (16),(17),(18) and (19) are presented in Figures 10 and 11; results for Van Leer and Roe fluxes again are supplied for comparison. The splitting parameters used were: $\mu = 1$, $\nu = \frac{3}{4}$, $\omega = 0$ and $P = 2$. It will be shown in the following section that this combination lies outside the stability range predicted by a stability analysis for inviscid flow. A converged solution was nevertheless obtained with the LU-SGS implicit marching scheme, while convergence could not be achieved with a single stage (forward Euler) explicit scheme. In fact, the results are the best obtained so

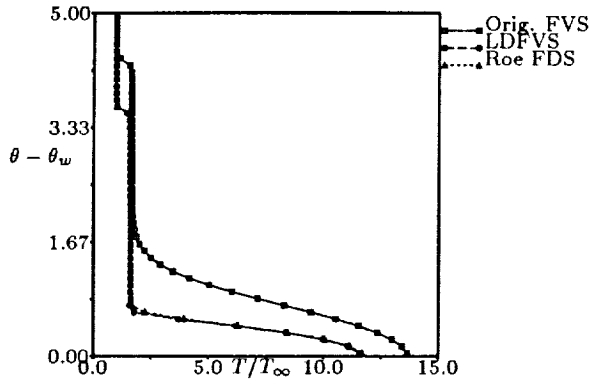


Figure 10: Conical Navier-Stokes solutions using the LDFVS formula for $\mu = 1$, $\nu = \frac{3}{4}$, $\omega = 0$, and $P = 2$; temperature distributions.

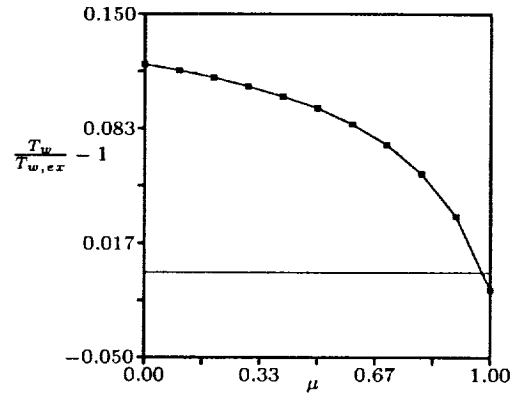


Figure 12: Error in computed wall temperature using various levels of μ for the conical Navier-Stokes solution.

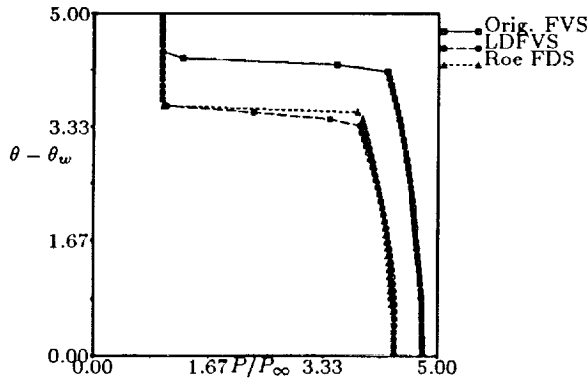


Figure 11: Same solutions as in Figure 10; pressure distributions.

far with a first-order scheme. Presumably this is so because the scheme reverts to central differencing wherever v is small, i.e. in the boundary layer. The wall temperature is essentially the same as for the Roe flux; the pressure curve actually is better than for Roe's flux, as it lacks the pressure dip apparent in the Roe results just above the boundary layer.

To illustrate the effect of μ upon the diffusive error in the solution, we then ran the same test problem for 11 values of μ combined with the optimum ν -value in the pres-

sure splitting as found from a stability analysis (Section 6), and $\omega = 0$. All of the computations were made with the LU-SGS scheme, and convergence to machine zero was obtained in 750 or fewer iterations. In Figure 12 the relative error in the wall temperature is plotted against μ , where the baseline wall temperature is found from

$$T_{w,ex} = T_{\infty} \left(1 + \sqrt{P_r} \frac{\gamma - 1}{2} M_{\infty}^2 \right) \quad (25)$$

The effect of the artificial diffusion is clear: for the uniform grid used, with about 8 cells in the boundary layer, the diffusion coefficient must be cut at least by an order of magnitude, i.e. $0.9 < \mu \leq 1$, in order to admit a wall temperature of acceptable accuracy.

Results obtained with the HOPE splitting, Equations (20), (21), (22) and (23), for the conical flow are presented and compared to other results in Figures 13 and 14. Since the mass, pressure and energy splittings are similar to those in the new FVS scheme, it is not surprising that the computed solutions are also very similar. Again, the LU-SGS scheme was used to converge the solution, and convergence to machine zero was obtained in ap-

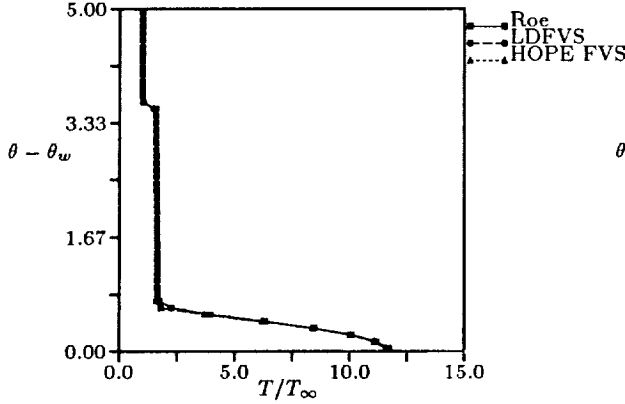


Figure 13: Conical Navier-Stokes solutions using the HOPE and LDFVS splittings: temperature distributions.

proximately 1000 iterations. Here too convergence could not be obtained using an explicit time-marching scheme. This stability behavior is also indicated by the stability analysis below.

It would appear from the above results for the one-dimensional conical flow that the new flux functions have potential for use in more realistic, multi-dimensional problems. This, however, turns out not to be true. To test the pure FVS schemes for a two-dimensional flow, the inviscid transonic flow about a NACA 0012 at 1.5° angle of attack and free-stream Mach number of $M = 0.85$ was computed on a relatively coarse (64 by 32 cell) grid. It was impossible to obtain any solution with either the LDFVS splitting ($\mu = 1$) or the HOPE splitting, regardless of Courant number or level of implicit dissipation (controlled by the splitting parameter in the LU-SGS scheme). For $\mu = 0.9$ a converged solution was obtained, although the resulting flowfield was highly non-monotone. To investigate this further, both fluxes were used to compute the $M = 2$ inviscid flow over a 10° compression ramp on a 50 by 50 cell grid. Both computa-

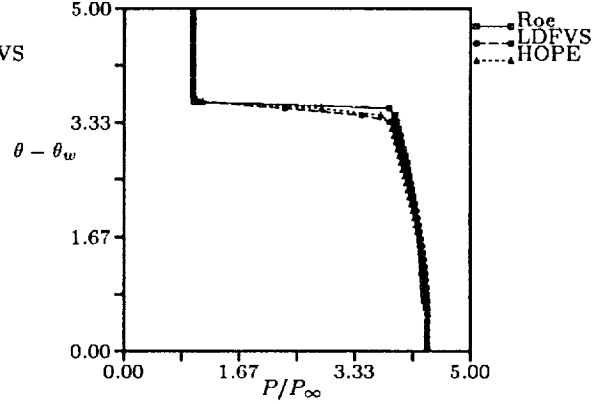


Figure 14: Same solution as Figure 13; Pressure distributions.

tions converged to machine zero, but yielded highly non-monotone results downstream of the ramp shock. This finding is discouraging, but not surprising, as the stability and monotonicity analysis in the following section will show. Note that this non-monotonicity occurred with *first-order* spatial differencing and can not be cured by the kind of limiters used in higher order schemes.

6 Stability and Monotonicity Analysis

The usual stability argument regarding FVS is that $\mathbf{B}^+ \equiv d\mathbf{F}^+/dU$ and $\mathbf{B}^- \equiv d\mathbf{F}^-/dU$ must have non-negative and non-positive eigenvalues, respectively, in keeping with the notion of forward and backward fluxes. This would be a necessary requirement if the two split-flux Jacobians would commute. It is hoped that by relaxing this requirement a stable and monotone FVS scheme could still be formed. We shall base our stability analysis on the first-order (cartesian) upwind-differencing operator

$$\Delta x \mathbf{Res} = -\{(\mathbf{F}_j^+ - \mathbf{F}_{j-1}^+)\}$$

$$+ (\mathbf{F}_{j+1}^- - \mathbf{F}_j^-) \} \quad (26)$$

with Fourier transform

$$\Delta x \Lambda(\beta, M) = - \left\{ \mathbf{B}^+ (1 - e^{-i\beta}) + \mathbf{B}^- (e^{i\beta} - 1) \right\}. \quad (27)$$

For stability of the differential equation

$$\frac{d\mathbf{U}}{dt} = \Lambda \mathbf{U} \quad (28)$$

all eigenvalues of Λ must have a non-positive real part; this must be enforced for all β and M .

In addition to stability, the split fluxes used in the discrete residual, (26), must yield monotone solutions of the state vector, \mathbf{U} . Consider the steady form of (26),

$$0 = \Delta_- \mathbf{F}^+ + \Delta_+ \mathbf{F}^- \quad (29)$$

This equation is then linearized resulting in

$$0 = \mathbf{B}^+ \Delta_- \mathbf{U} + \mathbf{B}^- \Delta_+ \mathbf{U} \quad (30)$$

or, for non-singular \mathbf{B}^-

$$0 = \mathbf{B} \Delta_- \mathbf{U} + \Delta_+ \mathbf{U}, \quad (31)$$

with

$$\mathbf{B} = (\mathbf{B}^-)^{-1} \mathbf{B}^+ \quad (32)$$

For a monotone solution, $\Delta_+ \mathbf{U}$ and $\Delta_- \mathbf{U}$ should have the same sign, so that the eigenvalues of \mathbf{B} must be all negative. As the eigenvalues of Λ and \mathbf{B} are difficult to obtain and study analytically, we shall resort to their numerical evaluation for the sake of carrying out the stability and monotonicity analyses.

First, we look at the stability properties of the LDFVS flux with a simple energy splitting. Figure 15 summarizes the stability properties of the spatial operator (26) incorporating the LDFVS splitting with $\gamma = 1.4$ and $\omega = 0$. For 11 values of μ , ranging from

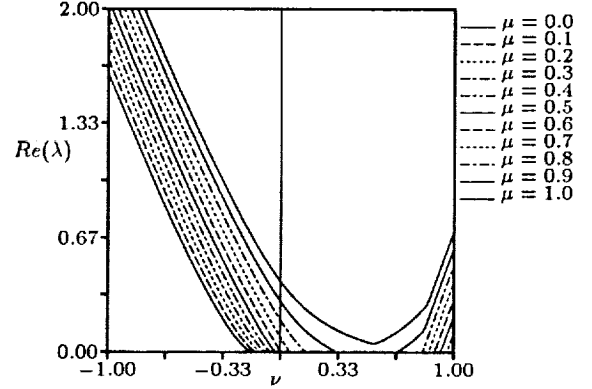


Figure 15: Maximum real part encountered in any of the eigenvalues of $\Lambda(\beta, M)$, versus ν , for a range of values of μ , using $P = 2$. The maximum is taken over all β and M .

0 to 1, the largest positive real part encountered among the three eigenvalues of $\Lambda(\beta, M)$ is plotted against ν . The eigenvalues of the matrix Λ were found numerically given the Mach and wave numbers using a packaged root solver.

For small values of μ there appears to be an appreciable range of ν -values for which no unstable eigenvalues occur. The stable range of ν narrows down considerably as μ increases, until only a single stable value of ν remains, i.e. $\nu = 0.52$ for $\mu = 0.96$. This shows that the diffusive fluxes at $M = 0$ can be reduced by a factor 25 without losing the possibility of being implemented in a stable time-marching scheme. Similar results, but slightly more restrictive, were obtained for $P = 6$, so this avenue was not explored further. We also checked stability for $\gamma = 1$, and found no qualitative difference.

Although this result is encouraging, it is desirable to make the scheme strictly stable for standard explicit procedures. For this we turn to the energy splitting and perform the stability analysis now for $\mu = 1$. Figure 16 shows the maximum of all eigenvalues (over

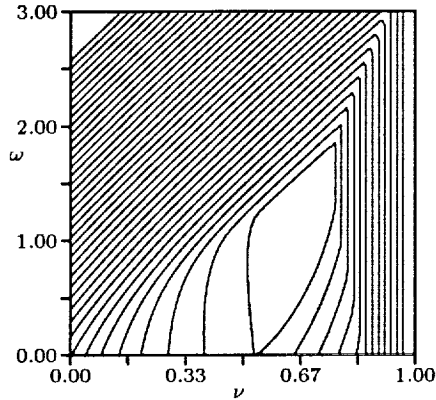


Figure 16: Contours of maximum real part of all eigenvalues for $\mu = 1$. The maximum is taken over all β and M . The lowest level displayed is 0.002.

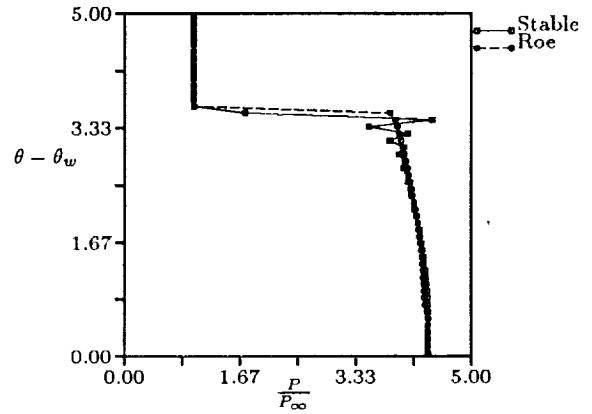


Figure 17: Conical Navier-Stokes solution using the stable splitting parameters: $\mu = 1.0$, $\nu = 3/4$ and $\omega = 3/2$.

all Mach and wave numbers) for selected values of both ν and ω . One can see that the scheme approaches stability in a very narrow trough with a minimum at $\nu = 3/4$ and $\omega = 3/2$, although even there the maximum eigenvalue is still slightly positive. This splitting is found to be stable in practice for the conical flow problem: for $\mu = 1$, $\nu = 3/4$ and $\omega = 3/2$ a converged solution can be obtained using a single-stage explicit (forward Euler) scheme with a Courant number of $CFL = 0.1$ after a large number (10,000) of iterations. Unfortunately, the stable LDFVS scheme yields the worst non-monotone solution for the conical flow, as is shown in Figure 17.

A detailed look at the eigenvalues is necessary to see if there is any hope at all of finding a scheme that will be both stable and monotone. Figure 18 shows the eigenvalues of \mathbf{B}^+ for the original FVS with Hänel's energy flux and the LDFVS for $\mu = 1$ and $\nu = \omega = 0$. This choice of parameters shows the effect of the low diffusion mass splitting upon the split flux eigenvalues. This Figure

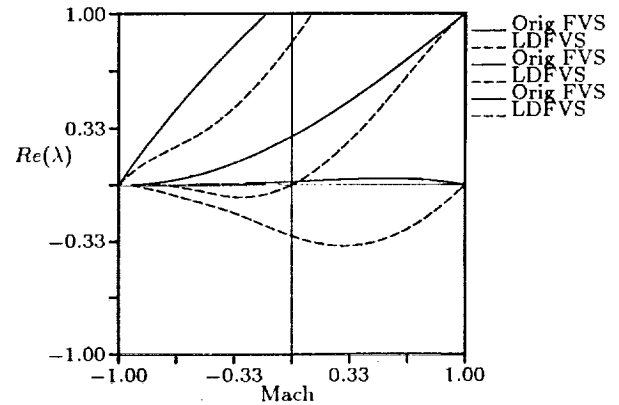


Figure 18: Eigenvalues of the forward-flux Jacobian, \mathbf{B}^+ , for the original FVS with Hänel's energy flux, and the LDFVS with $\mu = 1$, $\nu = \omega = 0$.

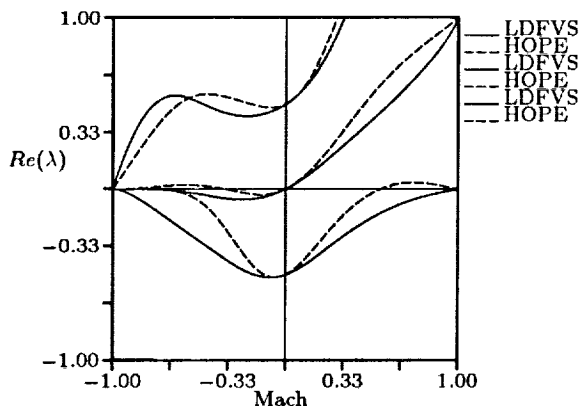


Figure 19: Eigenvalues of the forward-flux Jacobian, \mathbf{B}^+ , for the LDFVS with $\mu = 1$, $\nu = 3/4, \omega = 3/2$ and the HOPE FVS.

shows that the eigenvalue corresponding to the characteristic speed u has the incorrect sign for $M < 0$, while the eigenvalue corresponding to $u - a$, which for $M < 1$ should be zero or slightly positive, (in the context of a forward flux) has the wrong sign over the whole Mach number range. The stable splitting ($\mu = 1, \nu = 3/4$ and $\omega = 3/2$) and the HOPE splitting are compared in the next Figure. It is seen from this Figure that the eigenvalue corresponding to $u - a$ still has the incorrect sign over a large Mach number range for both splittings. With this type of behavior, it is highly unlikely that a monotone solution could generally be achieved with either of the non-diffusive fluxes, regardless of the pressure or energy splittings. This is also supported by the results of the full monotonicity analysis.

Figures 20, 21, 22, and 23 show the eigenvalues of \mathbf{B} over the range of Mach numbers $|M| < 1$. (These were computed by numerically finding the inverse of \mathbf{B}^- for $M < 0$, or \mathbf{B}^+ for $M > 0$, multiplying the inverse with the remaining Jacobian and finding the eigenvalues using a root solver.) The first figure

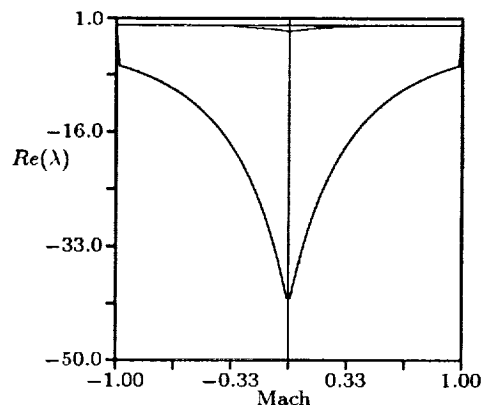


Figure 20: Eigenvalues of the \mathbf{B} matrix for the original FVS scheme using Hänel's energy flux.

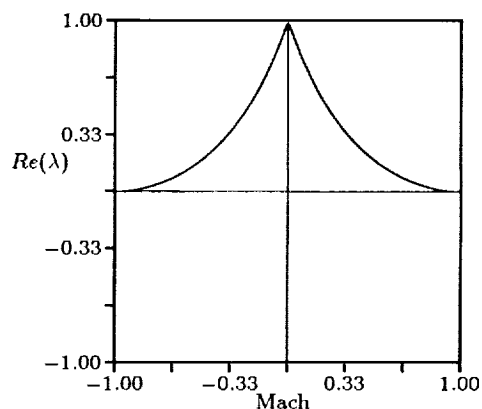


Figure 21: Eigenvalues of the \mathbf{B} matrix for the LDFVS splitting using $\mu = 1, \nu = \omega = 0$. The curves for all three eigenvalues fall nearly on top of each other.

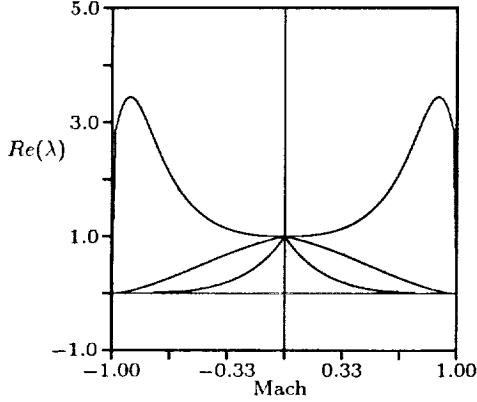


Figure 22: Eigenvalues of the \mathbf{B} matrix for the stable LDFVS splitting ($\mu = 1$, $\nu = 3/4$ and $\omega = 3/2$).

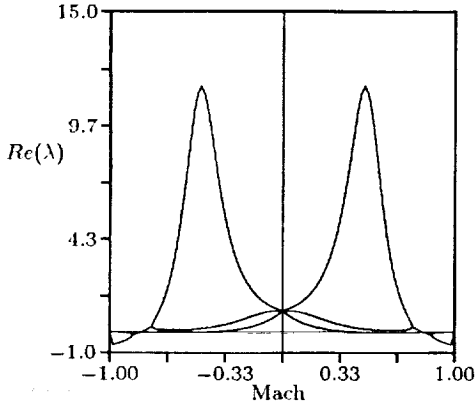


Figure 23: Eigenvalues of the \mathbf{B} matrix for the HOPE splitting.

shows the eigenvalues for the original FVS scheme. As can be seen here, all of the \mathbf{B} eigenvalues have the proper negative sign, as they should, which provides some level of confidence in the monotonicity argument. Figure 21 shows the eigenvalues of \mathbf{B} for the LDFVS with $\mu = 1$ and $\nu = \omega = 0$, while Figure 22 shows the eigenvalues for the stable LDFVS. Both of these schemes have all eigenvalues of \mathbf{B} of the wrong sign, which indicates that a monotone solution, whether stable or not, is generally impossible and a lucky coincidence at best. Figure 23 shows the eigenvalues for HOPE. Although it does have eigenvalues of the wrong sign over a wide range of Mach numbers, there is a region near $|M| = 1$ where the correct signs are observed. This behavior can be traced back to Figure 19, which shows the split flux eigenvalues. For a small region near $|M| = 1$ the HOPE scheme has the proper sign for all of the split-flux eigenvalues. But, as in the LDFVS schemes, the HOPE scheme has one eigenvalue that is hopelessly of the wrong sign near $M = 0$.

This type of behavior cannot be avoided, no matter what values are used for the parameters in LDFVS or HOPE, including the exponents P and S . The bottom line is that splittings that are non-diffusive for $M = 0$, by necessity must connect Van Leer's split fluxes for $|M| \rightarrow 1$ to central difference fluxes for $|M| \rightarrow 0$ (see Equations (12-15)), and the latter are known to yield oscillatory solutions.

7 Conclusions

In this paper we have compared various low-diffusion flux formulas for use in Navier-Stokes computations. To compare these various formulas, the viscous, hypersonic flow over a 10° cone at $M = 7.95$ was computed by solving the conical Navier-Stokes equations in one dimension. The Harten-Lax/Roe scheme, incorporating a "smart" scalar diffu-

sion coefficient, presented but not tested in [1], was tested here and shown to give good results, although there is some question as to its robustness. Next, recent developments in flux-vector and hybrid flux-vector/flux-difference splitting (FVS/FDS) were examined. These fluxes were shown to yield a correct temperature profile in the boundary layer, accompanied by a pressure irregularity near the boundary layer edge. In an attempt to overcome this deficiency, it was investigated whether a pure FVS could be constructed that would cause minimal dissipation across a contact discontinuity, yet still be stable and monotone. We have shown that it is indeed possible to construct a pure FVS scheme with minimal mass diffusion, although this is achieved at marginal stability and a loss of monotonicity, even for first-order spatial differencing. This makes pure FVS a dead-end street; the latest developments in hybrid FVS/FDS formulas, though, indicate that some elements of FVS may survive and be used advantageously in flux functions for the Navier-Stokes equations.

References

- [1] B. van Leer, J. L. Thomas, P. L. Roe, and R. W. Newsome, "A Comparison of Numerical Flux Formulas for the Euler and Navier-Stokes Equations," in *AIAA 8th Computational Fluid Dynamics Conference*, 1987.
- [2] B. van Leer, "Flux-vector Splitting for the Euler Equations," *Lecture Notes in Physics*, vol. 170, 1982.
- [3] A. Jameson, W. Schmidt, and E. Turkel, "Numerical solutions of the Euler equations by a finite-volume method using Runge-Kutta time-stepping schemes," AIAA Paper 81-1259, 1981.
- [4] P. L. Roe, "The use of the Riemann problem in finite-difference schemes," *Lecture Notes in Physics*, vol. 141, 1980.
- [5] R. C. Swanson and E. Turkel, "On central-difference and upwind schemes." ICASE Report 90-44, 1990.
- [6] M. S. Liou, B. van Leer, and J. S. Shuen, "Splitting of inviscid fluxes for real gases," *Journal of Computational Physics*, vol. 87, 1990.
- [7] M. Vinokur and Y. Liu, "Equilibrium gas flow computations II: An analysis of numerical formulations of conservation laws," AIAA Paper 88-0127, 1988.
- [8] B. Grossman and R. W. Walters, "Analysis of flux-split algorithms for Euler's equations with real gases," AIAA Paper 87-1117-CP, 1987.
- [9] C. L. Rumsey, B. van Leer, and P. L. Roe, "A grid-independent approximate Riemann solver with applications to the Euler and Navier-Stokes equations," AIAA Paper 91-0231, 1991.
- [10] C. L. Rumsey, B. van Leer, and P. L. Roe, "Effect of a multi-dimensional flux function on the monotonicity of Euler and Navier-Stokes computations," AIAA Paper 91-1530, 1991.
- [11] S. Obayashi and P. M. Goorjian, "Improvements and applications of a stream-wise upwind algorithm," in *AIAA 9th Computational Fluid Dynamics Conference*, 1989.
- [12] D. Hänel, R. Schwane, and G. Seider, "On the accuracy of upwind schemes for the solution of the Navier-Stokes equations," in *AIAA 8th Computational Fluid Dynamics Conference*, 1987.

- [13] D. Hänel and R. Schwane, "An implicit flux-vector splitting scheme for the computation of viscous hypersonic flow," AIAA Paper 89-0274, 1989.
- [14] B. van Leer, "Flux-vector splitting for the 1990's." Invited Lecture, NASA Lewis Research Center, 1990.
- [15] M.-S. Liou and C. Steffen Jr., "A New Flux Splitting Scheme," 1991. To be submitted.
- [16] S. Yoon and D. Kwak, "Artificial Dissipation Models for Hypersonic Internal Flow," AIAA Paper 88-3277, 1988.
- [17] A. Harten and P. Lax, "A Random Choice Finite Difference Scheme for Hyperbolic Conservation Laws," *SIAM J. Numer. Anal.*, vol. 18, pp. 289-315, 1981.
- [18] P. Roe, "Generalized Formulation of TVD Lax-Wendroff Schemes." NASA CR 172478, 1984.
- [19] M.-S. Liou and C. Steffen Jr., "A New Flux Splitting Scheme.." AIAA 10th. CFD Conference, 1991.
- [20] M. S. Liou and C. Steffen jr., "High-order polynomial expansions for flux-vector splitting." To be presented at the International Conference on Computational Engineering Science, 1991.



National Aeronautics and
Space Administration

Report Documentation Page

1. Report No. NASA TM -104353 AIAA-91-1566		2. Government Accession No.		3. Recipient's Catalog No.	
4. Title and Subtitle Numerical Flux Formulas for the Euler and Navier-Stokes Equations II. Progress in Flux-Vector Splitting				5. Report Date	
				6. Performing Organization Code	
7. Author(s) William J. Coirier and Bram van Leer				8. Performing Organization Report No. E -6138	
				10. Work Unit No. 505 -62-52	
9. Performing Organization Name and Address National Aeronautics and Space Administration Lewis Research Center Cleveland, Ohio 44135 - 3191				11. Contract or Grant No.	
				13. Type of Report and Period Covered Technical Memorandum	
12. Sponsoring Agency Name and Address National Aeronautics and Space Administration Washington, D.C. 20546 - 0001				14. Sponsoring Agency Code	
15. Supplementary Notes Prepared for the 10th Computational Fluid Dynamics Conference sponsored by the American Institute of Aeronautics and Astronautics, Honolulu, Hawaii, June 24-27, 1991. William J. Coirier, NASA Lewis Research Center; Bram van Leer, University of Michigan, Dept. of Aerospace Engineering, Ann Arbor, Michigan 48109. Responsible person, William J. Coirier, (216) 433-5885.					
16. Abstract The accuracy is studied of various numerical flux functions for the inviscid fluxes when used for Navier-Stokes computations. The flux functions are benchmarked for solutions of the viscous, hypersonic flow past a 10° cone at zero angle of attack using first-order, upwind spatial differencing. The Harten-Lax/Roe flux is found to give a good boundary layer representation, although its robustness is an issue. Some hybrid flux formulas, where the concepts of flux-vector and flux-difference splitting are combined, are shown to give unsatisfactory pressure distributions; there is still room for improvement. Investigations of low diffusion, pure flux-vector splittings indicate that a pure flux-vector splitting can be developed that eliminates spurious diffusion across the boundary layer. The resulting first-order scheme is marginally stable and not monotone.					
17. Key Words (Suggested by Author(s)) Numerical flux functions Navier-Stokes Flux vector splitting			18. Distribution Statement Unclassified - Unlimited Subject Category 02		
19. Security Classif. (of the report) Unclassified		20. Security Classif. (of this page) Unclassified		21. No. of pages 18	22. Price* A03